A Contact Finite Element Formulation for Biological Soft Hydrated Tissues

Peter S. Donzelli and Robert L. Spilker§

Department of Mechanical Engineering, Aeronautical Engineering and Mechanics

and Scientific Computation Research Center

§also Department of Biomedical Engineering

Rensselaer Polytechnic Institute, Troy, NY 12180-3590

Abstract

As part of the highly complex numerical simulation of human joints, a finite element formulation for contact between layers of articular cartilage has been developed. A biphasic description of the cartilage is used, where the material is considered to be a porous, permeable solid matrix with fluid flowing through it. Governing equations and contact boundary conditions are summarized for this material before developing the finite element formulation from a Galerkin weighted residual statement. Lagrange multipliers are introduced to enforce the two kinetic continuity equations across the contact surface, and an iterative scheme is employed to determine the current contact area. Numerical examples are presented which demonstrate both that the appropriate continuity across the contact surface is enforced and that the contact surface definition is accurate.

Introduction

With our population steadily aging, more and more adults are afflicted with osteoarthritis (OA). This is a degenerative disease affecting the articular cartilage in joints. When functioning normally, this cartilage provides a nearly frictionless bearing surface for the articulating bones [1,2]. As OA progresses, the cartilage changes mechanically, biochemically and structurally [3], compromising its performance. Overall, the causes of OA are not fully understood, but hypothesis have been put forth suggesting that repeated stressing of cartilage can eventually

lead to its degeneration [4]. To help explain the causes of OA, this research is concerned with understanding the mechanical response of articular cartilage layers in contact. A robust contact formulation is a crucial step toward developing a complete numerical simulation of human joint mechanics, which in turn can be used to investigate the complex clinical problems that effect cartilage degeneration and OA.

We choose the biphasic theory of Mow and co-workers [5] as the continuum description for articular cartilage and other soft hydrated tissues. The theory has been widely accepted as a means to model cartilage, and has been adopted by many other researchers in biomechanics (*i.e.* [6-8]). The theory has also been extended to include the nonlinearities observed in tissue mechanics, including finite deformation [9,10], strain-dependent permeability [11-13], transversely hyperelastic solid phase mechanics [14] or viscoelastic solid phase mechanics [15,16].

This section continues by citing those works in the literature that were most useful in developing the biphasic contact finite element, then subsequent sections present the governing equations and boundary conditions, the finite element formulation, details concerning contact surface calculations and lastly numerical examples to validate the present formulation.

There are two important considerations in choosing a biphasic contact finite element. First is the means by which the mixture continuity relation will be introduced into the formulation. It is well known that finite element formulations for constrained media problems can present significant difficulty when choosing the finite element interpolations [17,18], so particular care must be taken in choosing a robust element. Second is the method of enforcing the contact boundary conditions. The most common methods found in the literature are Lagrange multiplier methods, penalty function methods and augmented Lagrangians.

Regarding the continuity relation, there have been four methods reported for biphasic finite elements: the penalty formulation of Suh *et al.* [19,20], the mixed-penalty formulation of Spilker and Maxian [21], the hybrid formulation of Vermilyea and Spilker [22] and the pressure-velocity formulation of Oomens *et al.* [23] or the similar pressure-displacement formulation by Wayne *et al.* [24]. The penalty formulation of Suh was implemented for two

dimensional problems with a four-node quadrilateral. He notes that for distorted quadrilaterals, this element behaves poorly [25]. In addition, the mean dilatational formulation used for that element is not readily extensible to higher order elements, which are often desirable in constrained media problems. Maxian indicates these shortcomings as the motivation to develop the mixed-penalty element [26]. There is also strong motivation to use simplex elements when considering mesh generation on realistic geometries [27-29], or when employing adaptive mesh updates [30]. The pressure-velocity elements are quite attractive, since they replace the unknown fluid velocity in the formulation by the scalar pressure field, reducing the size of the assembled matrix equations. Both Oomens and Wayne note the well known tendency of velocity-pressure elements to show spatial oscillations when subjected to a step change in applied force. Oomens refers to the literature on consolidation in soil mechanics for further explanations of this phenomenon (for example, [31]). While these oscillations do diminish in time, they can have significant effects for nonlinear problems, or for solutions that take advantage of *h*-adaptive mesh enrichment.

The hybrid method has the advantage that it does not require the user to select a penalty parameter to enforce the continuity constraint. There are disadvantages, however, most significant being that the hybrid formulation requires a strain-stress law, as opposed to a stress-strain law for displacement-based elements. For linear materials it is straightforward to invert the material property matrix, but for nonlinear materials one must formulate the complimentary free energy function. While constitutive laws of this form could be constructed, experimentally curve fit to determine their parameters and tested to ensure physically plausible behaviour, one does not presently exist so biphasic studies to date with the hybrid element have been limited to linear analysis.

With these observations, then, the mixed-penalty element will be chosen as the basis on which to formulate the biphasic contact element. For reference, a complete presentation of the finite element equations is given by Spilker and Maxian [21]. This provides an accurate, efficient element which can be extended to nonlinear contact analysis in the future, and which has been successfully extended to model all relevant nonlinear mechanics for the single-region problem [32]. In addition, the element has been implemented for both triangles and tetrahedra,

allowing existing *h*-adaptive mesh enrichment schemes to be coupled to this formulation [30,33], providing the necessary resolution of moving contact interfaces.

Contact finite element formulations for linearly elastic and nonlinear materials, with and without friction, have been in use for nearly as long as the finite element method itself. They fall into the more general category of constraints applied to the finite element method, such as the constrained medial problems of incompressible solid or fluid mechanics. The text by Johnson [34] gives an extensive treatment of the contact problem in solid mechanics. Aspects of the numerical solution of contact problems by the finite element method are the subject the book by Kikuchi and Oden [35]. They give a complete discussion of the mathematical formalism behind contact finite elements, which leads them to a discussion of error estimates and the Babuska-Brezzi condition for constrained problems.

Dynamic contact, or contact-impact, has been treated by several authors, including Wriggers [36] and Belytschko [37]. An added effort is made to develop efficient computational algorithms in these strongly nonlinear, time-dependent problems. Wriggers proposes a frictional law from which a matrix form of the virtual work of the contact forces can be added directly to the finite element equations. This leads to a contact formulation in terms of displacement only, and no explicit constraint equations are introduced. The authors note that for some frictional laws, the method can be identified as a penalty method. Belytschko enforces impenetrability by examining the radii of 'pinballs' inscribed in the finite elements along with either penalty functions or Lagrange multipliers. He also notes that for an explicit central difference integration of the semi-descritized equations, the contact surface and Lagrange multipliers (interface tractions) can be determined without iteration.

Recently, researchers have embraced the method of perturbed or augmented Lagrangians as a computationally efficient means to enforce constraints on the finite element method. Simo and co-workers have applied the method to contact formulations. They first present the method as a way to regularize the ill-conditioned system that results from a Lagrange multiplier approach [38]. In the same publication, they present an unique treatment of the contact surface kinematics by contact *segments*. Simo and Laursen have extended that formulation

to include frictional effects on the contact surface [39]. Laursen and Oancea have indicated how the convergence characteristics of the augmented Lagrangian formulation render it superior to either penalty methods or Lagrange multipliers [40]. The advantage is that with finite penalties, there is nearly exact satisfaction of the constraint. On the other hand, it is not necessary to optimally choose the penalty to guarantee convergence. Heegaard has developed a large displacement, frictional sliding contact element for hyperelastic materials using the augmented Lagrangian approach [41,42]. He has applied this element to the problem of patello-femoral contact in the human knee, and has made comparisons of the numerical procedure to experimental results.

Governing Equations for Soft Tissue

This research is based upon the biphasic theory of Mow and co-workers [5], in which soft hydrated tissues are considered to be a continuum mixture of solid and fluid. Based on the observed structure of cartilage, several simplifying assumptions were used by Mow, *et al.* in their presentation of the theory [5]. First, both the solid and fluid phases are inert, and do not undergo any chemical changes or interactions. Each phase is considered incompressible, which gives rise to mass conservation statements for each phase, as well as for the mixture. For biological materials it is reasonable to assume isothermal deformations and no heat supply. Inertial terms are not included in this formulation and it is assumed that no energy is lost by convection across the contact surface [43].

A fully linear form of the governing biphasic equations is used for this development, where small strains are assumed, the solid phase is governed by a linear constitutive law, tissue permeability is constant and volume fractions of the solid and fluid phase do not change with deformation. Correlations of theoretical results with one-dimensional confined compression tests suggest that these assumptions are valid in a wide range of problems, including up to nearly 20% compressive strain in the solid matrix [5].

Governing differential equations for the theory are derived from integral statements of balance of mass, momentum and energy. Contact boundary conditions are found in the same way, but with integrals performed over a volume having a surface of discontinuity, as first reported for the biphasic theory by Hou *et al.* [43]. This results in the theoretically correct statement of traction continuity and relative flow across the interface. An additional

assumption of frictionless contact is introduced for the present work, as motivated by experimental findings [1,2]. This provides a significant simplification in the boundary conditions, since tangential components of traction can be eliminated from the expressions. In solving a contact problem by the finite element method the solution procedure is nonlinear, since the contact area is unknown in advance. This is true even in the case of fully linear constitutive relations and small strains. Additional restrictions beyond the contact boundary conditions must be imposed to recover an unique solution to this nonlinear problem.

This derivation considers two continuum bodies, denoted body 'A' and body 'B'. Extensions to multiple-body contact are straightforward and are treated within the numerical procedure. The contact surface is defined by the relation $\Gamma_c \equiv \Omega^A \cap \Omega^B$ and the fact that it must satisfy $\Gamma_c \subset \Re^{n_{sd}-1}$ with $\Omega^A \subset \Re^{n_{sd}}$ and $\Omega^B \subset \Re^{n_{sd}}$, where n_{sd} is the number of spatial dimensions in the problem. At times, to emphasize terms associated with either body 'A' or body 'B', the notation $\Gamma_c \cap \Omega^A$ will be used, although this intersection merely recovers the contact surface. Standard indicial notation is used, so summation is implied by the repeated indices i, j, k or m. Subscripts represent components and range 1, 2 ... n_{sd}; superscripts 'A' and 'B' refer to the body with which a given quantity is associated. This geometry is depicted in Fig. 1.

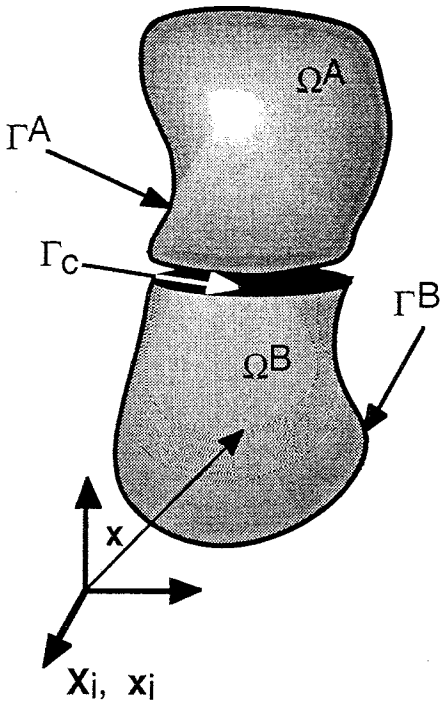

Fig. 1: Problem domain for contact between two deformable, biphasic continua.

The system of differential equations to which the finite element method will be applied are [5] the continuity relation for the mixture,

$$\left(\phi^s v_i^s + \phi^f v_i^f\right)_{,i} = 0, \tag{1}$$

and the momentum equations for the solid and fluid phases,

$$\sigma_{ij,j}^{\alpha} + \Pi_i^{\alpha} = 0, \quad \alpha = s,f, \tag{2}$$

where ϕ^{α}, $\alpha = s,f$, are the volume fractions of solid and fluid, $\mathbf{v}^{\alpha}$ are the phase velocities, σ^{α} are the Cauchy stress tensors and Π^{α} are vectors of diffusive momentum exchange. Note that for a saturated mixture, $\phi^s + \phi^f = 1$. There are three constitutive laws to govern the momentum exchange and stress-strain behaviour:

$$\Pi_i^s = -\Pi_i^f = p\,\phi_{,i}^s + K(v_i^f - v_i^s), \tag{3a}$$

$$\sigma_{ij}^s = -\phi^s\, p\,\delta_{ij} + D_{ijkm}^s \varepsilon_{km}^s, \tag{3b}$$

$$\sigma^{f}_{ij} = -\phi^{f}\, p\, \delta_{ij} + D^{f}_{ijkm}\, \overset{\circ}{\varepsilon}{}^{f}_{km}, \tag{3c}$$

where $K = \dfrac{\phi^{f2}}{\kappa}$ is a diffusive drag coefficient [12], κ is the tissue permeability, p is the interstitial pressure, ε^{s} is solid strain and $\overset{\circ}{\varepsilon}{}^{f}$ is fluid strain rate. These are derived with the previously stated assumptions on small deformations, constant permeability and volume fractions constant in time. The fourth rank tensors $\mathbf{D}^{\alpha}$ admit orthotropic behaviour, but are not dependent on deformation. In applying the assumption of frictionless contact to simplify the contact boundary conditions, viscous effects of the fluid have been ignored, so non-zero values of $\mathbf{D}^{f}$ are precluded. The contact continuity relations developed by Hou and co-workers [43] are manipulated to introduce the assumption of frictionless contact, and to isolate the kinematic and kinetic terms [44], yielding:

$$(u_i^{sA} + X_i^{sA})\, n_i^{A} + (u_i^{sB} + X_i^{sB})\, n_i^{B} = 0, \tag{4a}$$

$$\left(\phi^{fA}\,(u_i^{fA} + X_i^{fA}) + \phi^{sA}\,(u_i^{sA} + X_i^{sA})\right) n_i^{A} +$$

$$+ \left(\phi^{fB}\,(u_i^{fB} + X_i^{fB}) + \phi^{sB}\,(u_i^{sB} + X_i^{sB})\right) n_i^{B} = 0. \tag{4b}$$

$$\frac{(\sigma_{ik}^{fA}\, n_i^{A}\, n_k^{A})}{\phi^{fA}} - \frac{(\sigma_{ik}^{fB}\, n_i^{B}\, n_k^{B})}{\phi^{fB}} = 0, \tag{4c}$$

$$(\sigma_{ik}^{sA}\, n_i^{A}\, n_k^{A}) - (\sigma_{ik}^{sB}\, n_i^{B}\, n_k^{B}) - \frac{\phi^{sA}}{\phi^{fA}}\,(\sigma_{ik}^{fA}\, n_i^{A}\, n_k^{A}) + \frac{\phi^{sB}}{\phi^{fB}}\,(\sigma_{ik}^{fB}\, n_i^{B}\, n_k^{B}) = 0, \tag{4d}$$

where $\mathbf{n}$ is an external normal to the contact surface. Interpreted with respect to the linear constitutive relations the above represent continuity of normal solid velocity, continuity of normal relative fluid flow, continuity of pressure and continuity of normal elastic traction. Observe that Eqns. (4a,b) are expressed in terms of displacements, $\mathbf{u}^{\alpha}$, and reference position, $\mathbf{X}^{\alpha}$. For points in persistent contact, the time derivatives of these expressions gives the continuity of velocity, while at the instant of contact they provide a necessary forcing term proportional to the initial separation of the points. There are two kinematic, or essential, boundary conditions for biphasic materials:

$$v_i^{s} = \bar{v}_i^{s} \quad \text{on } \Gamma_{v_i}s, \tag{5a}$$

$$v_i^{f} = \bar{v}_i^{f} \quad \text{on } \Gamma_{v_i}f, \tag{5b}$$

and two kinetic, or natural, boundary conditions

$$\sigma^{s}_{ij} n_j = t^{s}_i = \bar{t}^{s}_i \text{ on } \Gamma_{t^s_i}, \tag{6a}$$

$$\sigma^{f}_{ij} n_j = t^{f}_i = \bar{t}^{f}_i \text{ on } \Gamma_{t^f_i}. \tag{6b}$$

Initial conditions are also required for this first order differential system in time, and so displacement and velocity are chosen to be zero at t = 0. There are three additional relations required to uniquely determine the correct contact area. The Kuhn-Tucker conditions of optimality [45] for a contact problem state that anywhere on the material boundary:

$$||\mathbf{g}(\mathbf{s})|| \leq 0, \tag{7a}$$

$$\mathbf{t}^{T}(\mathbf{s}) \bullet \mathbf{n}(\mathbf{s}) \leq 0, \tag{7b}$$

$$||\mathbf{g}(\mathbf{s})|| \quad \mathbf{t}^{T}(\mathbf{s}) \bullet \mathbf{n}(\mathbf{s}) = 0, \tag{7c}$$

where $\mathbf{g}(\mathbf{s})$ is closest point projection to an opposing surface, $\mathbf{t}^{T}(\mathbf{s})$ is the total traction vector and $\mathbf{s}$ is a surface coordinate. These are also the familiar boundary inequalities that result from the Signorini problem for linear elasticity (see, for example, [35]). These relations are intuitive, since a free surface must be traction-free and have a positive distance to an opposing surface, and since bodies in contact must experience a compressive surface traction.

Finite Element Formulation

The finite element method has a rich history which began when researchers in the 1950's began to apply relaxation and approximation methods to structural problems. A tremendous mathematical formalism has been developed since then, which allows nearly any system of equations to be approximated. Before the biphasic finite element equations can be developed, however, two important steps must be taken. First, the mixture continuity equation and contact boundary conditions must be modified to facilitate the numerical procedure. Second, since we will develop our finite element equations from a weighted residual statement, a precise mathematical statement of the function spaces in which solutions will be sought is required. Then a weak form of the problem can be formulated, to which the numerical approximation will be applied.

Preliminaries

The weighted residual statement is constructed from the governing equations and natural boundary conditions in each domain, and from the contact boundary conditions. In particular, the solid and fluid momentum equations, a penalized form of the mixture continuity relation and the traction boundary conditions will be approximated, while the constitutive laws, strain-displacement relations and essential boundary conditions will be exactly satisfied. The method begins by developing a penalized form of the continuity equation [21,46],

$$\left(\phi^s v_i^s + \phi^f v_i^f\right)_{,i} + \frac{p}{\beta} = 0, \tag{8}$$

which in the limit $\beta \rightarrow \infty$ is equivalent to the original continuity relation. Suh developed a methodology to estimate the penalty parameter for the biphasic equations [25]. He found the penalty parameter was proportional to machine accuracy, a reference time and the equilibrium modulus of the solid phase, and inversely proportional to volume fraction. He also demonstrated that for linear problems, the penalty parameter can be varied over approximately four orders of magnitude with no adverse effect on the solution.

Lagrange multipliers are typically used to append constraints to a variational principle, however, in the absence of an energy functional in the biphasic case, it is still possible to develop finite element equations which represent a Lagrange multiplier constraint operation. To introduce the contact boundary conditions into the weighted residual statement, and still retain the properties of a Lagrange multiplier method, it is necessary to redefine the kinetic contact continuity relations. If the finite element equations which result from a weighted residual statement are symmetric, one can conclude that a functional does exist which produces the same finite element equations [47]. In addition, the Euler equations of this unknown functional are precisely those equations introduced into the weighted residual statement. Thus, in this formulation, the kinetic continuity relations will be rewritten to define the Lagrange multipliers according to analogies with contact formulations for single phase solid mechanics and the Principle of Minimum Potential Energy. For the biphasic case two scalar multipliers will be required: one each for the solid and fluid kinetic contact continuity relations. From Eq. (4c) define λ^f on the contact surface and require:

$$\lambda^f = \frac{\sigma_{ij}^{fA}\, n_i^A\, n_j^A}{\phi^{fA}} \quad \text{on } \Omega^A \cap \Gamma_c, \tag{9a}$$

$$\lambda^f = \frac{\sigma_{ij}^{fB}\, n_i^B\, n_j^B}{\phi^{fB}} \quad \text{on } \Omega^B \cap \Gamma_c. \tag{9b}$$

In a similar manner, define λ^s on the contact surface from Eq. (4d):

$$\lambda^s = (\sigma_{ij}^{sA}\, n_i^A\, n_j^A) - \frac{\phi^{sA}}{\phi^{fA}} (\sigma_{ij}^{fA}\, n_i^A\, n_j^A) \quad \text{on } \Omega^A \cap \Gamma_c, \tag{10a}$$

$$\lambda^s = (\sigma_{ij}^{sB}\, n_i^B\, n_j^B) - \frac{\phi^{sB}}{\phi^{fB}} (\sigma_{ij}^{fB}\, n_i^B\, n_j^B) \quad \text{on } \Omega^B \cap \Gamma_c. \tag{10b}$$

Note that λ^s and λ^f are not independent in body 'A' and body 'B', but rather are defined on Γ_c such that they enforce the continuity required by Eqns. (4c,d). They become additional variables which must be interpolated in the finite element formulation, and from which the normal components of interface tractions can be recovered.

Choice of Trial and Test Spaces

The essence of the weighted residual method is to multiply each equation that will be approximated by an arbitrary weighting function, integrate this over the domain where the equation is to be enforced and sum these. For arbitrary weight functions, the resulting weighted sum is equivalent to the governing equations [48]. For the biphasic contact element, three classes of weight, or test, functions are required. These function spaces are defined as follows:

$$\vartheta_v = \left\{ w \mid w \in H^1 \text{ and } w = 0 \text{ on } \Gamma_{vs} \cup \Gamma_{vf} \right\}, \tag{11a}$$

$$\vartheta_p = \left\{ w \mid w \in H^0 \right\}, \tag{11b}$$

$$\vartheta_c = \left\{ w \mid w \in H^0 \text{ and } w = 0 \text{ on } \Omega \backslash \Gamma_c \right\}, \tag{11c}$$

where H^s are Sobolev spaces equipped with their natural norms. Respectively, these will be spaces of velocity, pressure and contact weight functions. These are, in effect, smoothness requirements on the test functions, and will

ensure that the subsequent mathematical manipulations are well defined. Additionally, three function spaces for the trial solutions must be defined as

$$\delta_{v_i}^{\alpha} = \left\{ w \mid w \in H^1 \text{ and } w = \bar{w} \text{ on } \Gamma_{v_i}^{\alpha} \right\}, \quad \alpha = s,f, \tag{12a}$$

$$\delta_p = \left\{ w \mid w \in H^0 \right\}, \tag{12b}$$

$$\delta_c = \left\{ w \mid w \in H^0 \text{ and } w = 0 \text{ on } \Omega \backslash \Gamma_c \right\}. \tag{12c}$$

Analogous to the test functions, these are trial spaces for the velocity (or displacement), pressure and Lagrange multipliers. These definitions require that the trial solutions satisfy the essential boundary conditions, while the velocity weight functions need only satisfy the homogeneous form of the essential boundary conditions. Rigorously, the space of velocities must also be constrained by the kinematic part of the Kuhn-Tucker relations, Eq. (7a) [35]. In practice, this requirement is too strong, since the deformed state of the material is unknown in advance. Alternatively, an iterative procedure has been developed which finds solutions satisfying both Eqns. (7) and (12).

Development of the Weak Form

A single weighted residual statement will be written as the sum of terms from body 'A', body 'B' and the contact surface, such that

$$G^A + G^B + G^c = 0. \tag{13}$$

For clarity, each of these will be presented separately. From body 'A' the contributions to the weighted residual come from the momentum equations, traction boundary conditions, penalized continuity equation and Lagrange multiplier definitions:

$$G^A = \int_{\Omega^A} w_i^{sA} (\sigma_{ij,j}^{sA} + \Pi_i^{sA}) d\Omega + \int_{\Gamma_{ti}^{sA}} h_i^{sA} (\bar{t}_i^{sA} - t_i^{sA}) \, d\Gamma +$$

$$+ \int_{\Omega^A} w_i^{fA} (\sigma_{ij,j}^{fA} + \Pi_i^{fA}) d\Omega + \int_{\Gamma_{ti}^{fA}} h_i^{fA} (\bar{t}_i^{fA} - t_i^{fA}) \, d\Gamma +$$

$$+ \int_{\Omega^A} w^{cA} \left(\left(\phi^{fA} v_i^{fA} + \phi^{sA} v_i^{sA} \right)_{,i} + \frac{p^A}{\beta^A} \right) d\Omega +$$

$$+ \int_{\Gamma_c} r^{fA} \left(\lambda^f - \frac{\sigma_{ij}^{fA} n_i^A n_j^A}{\phi^{fA}} \right) d\Gamma +$$

$$+ \int_{\Gamma_c} r^{sA} \left(\lambda^s - (\sigma_{ij}^{sA} n_i^A n_j^A) + \frac{\phi^{sA}}{\phi^{fA}} (\sigma_{ij}^{fA} n_i^A n_j^A) \right) d\Gamma. \tag{14}$$

Here the requirements on the weight functions are that $w_i^\alpha \in \vartheta_v$, $h_i^\alpha \in \vartheta_v$, $r^\alpha \in \vartheta_v$ and $w^c \in \vartheta_p$ for $\alpha = s,f$. Trial solutions are restricted to be members of the spaces defined by Eqns. (12) as follows: $v_i^\alpha \in \delta_{v_i^\alpha}$, $p \in \delta_p$ and $\lambda^\alpha \in \delta_c$. Observe that Eq. (14) contains the definitions of the multipliers given by Eqns. (9a) and (10a). The contributions from body 'B' are similar and, in particular, the requirements for trial and test spaces for the solution and weight functions are the same. Terms in the weighted residual from the contact surface are

$$G^c = \int_{\Gamma_c} \frac{s^s}{\Delta t \, \omega} \left((u_i^{sA} + X_i^{sA}) n_i^A + (u_i^{sB} + X_i^{sB}) n_i^B \right) d\Gamma +$$

$$+ \int_{\Gamma_c} \frac{s^f}{\Delta t \, \omega} \left[\left(\phi^{fA} (u_i^{fA} + X_i^{fA}) + \phi^{sA} (u_i^{sA} + X_i^{sA}) \right) n_i^A + \right.$$

$$\left. + \left(\phi^{fB} (u_i^{fB} + X_i^{fB}) + \phi^{sB} (u_i^{sB} + X_i^{sB}) \right) n_i^B d\Gamma \right], \tag{15}$$

and come from Eqns. (4a,b). The contact weight factors are restricted to be in H^o: $s^\alpha \in \vartheta_c$ for $\alpha = s,f$. The decision to scale the scalar weight functions will become apparent after the time discretization. Of course, since this is an arbitrary weight function, the scale factor does not effect the generality of this derivation.

Element Interpolations

At this stage the weak form is developed by applying the divergence theorem to terms containing the divergence of stress, and by choosing appropriate relations among the weight functions. It is important to note that the weak form is equivalent to the governing equations, and no approximations have been introduced. The next step is to chose finite-dimensional counterparts to the function spaces given in Eqns. (11-12), which will suggest the numerical approximation. This will be conducted in a formal way, producing a set of matrix equations valid for acceptable choices of interpolations in two or three dimensions. The final step is to particularize the interpolations for a six-node, triangular element.

The domain is divided into elements and the kinematic variables, pressure, Lagrange multipliers (λ^s and λ^f) and weight functions are interpolated in terms of their element nodal values, with subscript 'e' indicating the element number. The interpolations within element 'e' are chosen as follows. Solid and fluid velocity are interpolated with functions, $\mathbf{N} \in \delta^h_{v\alpha} \subset \delta_{v\alpha}$, where the superscript 'h' refers to the finite-dimensional subset. The form of the interpolation for velocity is

$$\mathbf{v}^{\alpha\gamma} = \mathbf{N}\, \mathbf{v}_e^{\alpha\gamma}, \quad \alpha = s,f \quad \gamma = A,B, \tag{16a}$$

and for solid displacement is

$$\mathbf{u}^{s\gamma} = \mathbf{N}\, \mathbf{u}_e^{s\gamma}, \quad \gamma = A,B, \tag{16b}$$

where the coefficients $\mathbf{u}_e^{s\gamma}$ are related to $\mathbf{v}_e^{s\gamma}$ by a time derivative. The velocity weight functions which, for a Galerkin weighted residual method, have the same polynomial form as the velocities, are interpolated with functions $\mathbf{N} \in \vartheta^h_v \subset \vartheta_v$ as

$$\mathbf{w}^{\alpha\gamma} = \mathbf{N}\, \mathbf{w}_e^{\alpha\gamma}, \quad \alpha = s,f \quad \gamma = A,B. \tag{16c}$$

Referring to the definitions of the spaces in Eqns. (11-12), the only difference in the interpolations for the velocity and its weight functions are at locations where essential boundary conditions are specified. This has the effect of removing as independent equations those corresponding to the constrained degrees of freedom, and producing

additional forcing terms related to the essential conditions. With this recognized, the slight abuse in notation of using the same symbol for both the velocity and its weight function will be allowed. In the computer implementation, this distinction is properly accounted for by an element-level constraint operation. Pressure is interpolated with functions $\mathbf{N}_p \in \delta_p^h \subset \delta_p$ as

$$p^\gamma = \mathbf{N}_p \, p_e^\gamma, \quad \gamma = A,B, \tag{16d}$$

and its weight function with $\mathbf{N}_p \in \vartheta_p^h \subset \vartheta_p$ as

$$w^{c\gamma} = \mathbf{N}_p \, w_e^{c\gamma}, \quad \gamma = A,B. \tag{16e}$$

Each of these two interpolations has a lower order continuity than the velocity. The solid and fluid multipliers, whose interpolant is non-zero only on the contact surface, are interpolated with functions $\mathbf{M} \in \delta_c^h \subset \delta_c$ as

$$\lambda^\alpha = \mathbf{M} \, \lambda_e^\alpha, \quad \alpha = s,f, \tag{16f}$$

and the corresponding weight function with $\mathbf{M} \in \vartheta_c^h \subset \vartheta_c$ as

$$s^\alpha = \mathbf{M} \, s_e^\alpha, \quad \alpha = s,f. \tag{16g}$$

Element reference coordinates, required in the kinematic contact continuity relations, are interpolated in the same way as displacement,

$$\mathbf{X}^{\alpha\gamma} = \mathbf{N} \, \mathbf{X}_e^{\alpha\gamma}, \quad \alpha = s,f \quad \gamma = A,B. \tag{16h}$$

Last is an interpolation for the known volume fraction,

$$\phi^{\alpha\gamma} = \tilde{\mathbf{N}} \, \phi_e^{\alpha\gamma}, \quad \alpha = s,f \quad \gamma = A,B, \tag{16i}$$

enabling the numerical calculation of the gradient of volume fraction within the finite element program. The interpolation matrix $\tilde{\mathbf{N}}$ would typically contain the same polynomials as $\mathbf{N}$, though the ordering within the matrix is different.

At this time the constitutive relations are substituted into the weak form, which necessitates several other definitions. Strain and strain rate are defined as the symmetric part of the gradient of solid displacement and fluid velocity, respectively, and are interpolated as,

$$\varepsilon^s = \nabla^s \mathbf{N}\, \mathbf{u}_e^s = \mathbf{B}\, \mathbf{u}_e^s \tag{17a}$$

$$\overset{\circ}{\varepsilon}{}^f = \nabla^s \mathbf{N}\, \mathbf{v}_e^f = \mathbf{B}\, \mathbf{v}_e^f, \tag{17b}$$

with ∇^s the symmetric gradient operator. Similar operations are performed for the symmetric gradient of the weighting functions. The gradient of volume fraction,

$$\nabla\phi^{\alpha\gamma} = \nabla\tilde{\mathbf{N}}\, \phi_e^{\alpha\gamma} = \tilde{\mathbf{B}}\, \phi_e^{\alpha\gamma}, \quad \alpha = s,f \quad \gamma = A,B, \tag{18a}$$

is required in terms coming from the momentum exchange and continuity relation. Because the mixture is saturated, gradients of the solid and fluid volume fractions are related,

$$\nabla\phi^{f\gamma} = \nabla(1 - \phi^{s\gamma}) = -\nabla\phi^{s\gamma}, \quad \gamma = A,B. \tag{18b}$$

In the finite element method, a reduced index notation will be used for stress and strain, where the independent terms of the symmetric tensors are arranged in a vector. To account for this, the vector **m** is defined as the reduced index form of the Kronecker delta operator, and the fourth rank tensors of material properties are redefined accordingly.

These interpolations are substituted into the weak form and the pressure, since it is interpolated with C^{-1} functions, is eliminated at the element level yielding the following matrix differential equations:

$$\sum_{e=1}^{n_{el}} \begin{Bmatrix} w_e^A \\ w_e^B \\ \dfrac{s_e}{\omega\Delta t} \end{Bmatrix}^T \begin{bmatrix} C_e^A + ß_e^A & 0 & Q_e^A \\ 0 & C_e^B + ß_e^B & Q_e^B \\ 0 & 0 & 0 \end{bmatrix} \begin{Bmatrix} v_e^A \\ v_e^B \\ \lambda_e \end{Bmatrix} +$$

$$+\sum_{e=1}^{n_{el}} \begin{Bmatrix} w_e^A \\ w_e^B \\ \dfrac{s_e}{\omega\Delta t} \end{Bmatrix}^T \begin{bmatrix} K_e^A & 0 & 0 \\ 0 & K_e^B & 0 \\ Q_e^{A^T} & Q_e^{B^T} & 0 \end{bmatrix} \begin{Bmatrix} u_e^A \\ u_e^B \\ 0 \end{Bmatrix} =$$

$$= \sum_{e=1}^{n_{el}} \begin{Bmatrix} w_e^A \\ w_e^B \\ \dfrac{s_e}{\omega\Delta t} \end{Bmatrix}^T \begin{Bmatrix} f_e^A \\ f_e^B \\ g_e \end{Bmatrix} \tag{19}$$

The matrices **C**, **ß** and **K** are discrete forms of the momentum exchange and fluid stiffness, penalized continuity, and solid stiffness, respectively, while the vectors **f** and **g** are due to prescribed tractions and initial separation on the contact surface. The contact coupling matrices are of particular interest here and have the form

$$\mathbf{Q}_e^\gamma = \begin{bmatrix} \mathbf{q}_e^\gamma & \phi^{s\gamma}\mathbf{q}_e^\gamma \\ \mathbf{0} & \phi^{f\gamma}\mathbf{q}_e^\gamma \end{bmatrix}, \quad \gamma = \text{A,B}, \tag{20a}$$

with

$$\mathbf{q}_e^\gamma = -\int_{\Gamma_{c_e}} \mathbf{N}^T \mathbf{n}^\gamma \mathbf{M}\, d\Gamma, \quad \gamma = \text{A,B}. \tag{20b}$$

Recognize that this matrix is often null since the integral is zero for elements which do not lie on the contact surface. It is also interesting to note that the matrix $\mathbf{q}$ is precisely that which arises in a Lagrange multiplier formulation for single phase elasticity. This matrix couples the multipliers to degrees of freedom on both sides 'A' and 'B' of the interface. In the biphasic case, the matrix **Q** performs this coupling, including the cross coupling between solid and fluid degrees of freedom on opposite sides of the contact surface.

Before assembling the global counterpart of Eq. (19), the family of generalized trapezoidal finite difference rules is applied in time [48]. For the present implementation, the time scale of the problem is divided into uniform increments of length Δt, and the displacement at the current time step is written in terms of the current velocity and the displacements and velocities at the previous time step,

$$\mathbf{u} = \hat{\mathbf{u}} + \Delta t\,(1-\omega)\,\hat{\mathbf{v}} + \Delta t\,\omega\,\mathbf{v}. \tag{21}$$

The superposed (^) indicates the known value at the previous time step and ω is an user-defined parameter chosen between 0 and 1 that controls the order of accuracy of the time integration, numerical damping, *etc.* When $\omega \geq 0.5$ the integration corresponds to an implicit method which is stable for any size time step. Equation (21) is substituted into Eq. (19) and the known values are transferred to the right hand side. Standard finite element assembly procedures are now applied to this system, and the assembled weight functions are recognized as arbitrary, which leads to a global system of equations,

$$\begin{aligned}
&\left\{\begin{bmatrix} C^A + ß^A & 0 & Q^A \\ 0 & C^B + ß^B & Q^B \\ Q^{A^T} & Q^{B^T} & 0 \end{bmatrix} + \omega\Delta t \begin{bmatrix} K^A & 0 & 0 \\ 0 & K^B & 0 \\ 0 & 0 & 0 \end{bmatrix}\right\}\begin{Bmatrix} v^A \\ v^B \\ \lambda \end{Bmatrix} = \\
&= \begin{Bmatrix} f^A \\ f^B \\ \dfrac{g}{\omega\Delta t} \end{Bmatrix} - \begin{bmatrix} K^A & 0 & 0 \\ 0 & K^B & 0 \\ \dfrac{Q^{A^T}}{\omega\Delta t} & \dfrac{Q^{B^T}}{\omega\Delta t} & 0 \end{bmatrix}\begin{Bmatrix} \hat{u}^A + \Delta t(1-\omega)\hat{v}^A \\ \hat{u}^B + \Delta t(1-\omega)\hat{v}^B \\ 0 \end{Bmatrix}
\end{aligned}, \tag{22}$$

where the matrices without the subscript 'e' are the assembled counterparts of those with the 'e'. This is a semi-definite system as is typical of Lagrange multiplier methods. Note that as the contact surface evolves in this linear problem, only the matrices $\mathbf{Q}^A$ and $\mathbf{Q}^B$ will change, so for a direct solution strategy the upper 2x2 block of Eq. (22) need be factored only once.

For the first mixed-penalty biphasic contact finite element, the computer implementation is restricted to the six-node, quadratic-velocity triangle, as first developed for single-region problems by Spilker and Maxian [21]. Thus, interpolations for displacement and velocity are quadratic, and use the familiar Lagrangian shape functions for

the triangle [48]. Both a plane strain and an axisymmetric version of the element have been implemented. The element is isoparametric, and has nodes at the vertices and mid-edges. All calculations are performed in the element parent coordinate system, which is based on triangular area coordinates. Gaussian quadrature of sufficient order to exactly integrate straight-sided elements is performed for all element matrices. The pressure interpolation is linear within an element, and independent from element to element, as would be expected for this constrained media problem. Maxian found that a three-parameter interpolation written directly in terms of the triangular coordinates produced a matrix that was insensitive to numerical instability during inversion [26].

If the finite element matrices are to be symmetric, which is an highly desirable characteristic, the Lagrange multipliers and contact weight functions must be interpolated with the same functions. Referring to the weighted residual, Eqns. (13-15), one should choose the interpolant such that there are as many independent coefficients in the contact weight function as there are in the velocity. This is a quadratic interpolation and would produce solutions where the weighted integral form of the kinematic contact continuity relations are exactly enforced. This choice favors a more rigorous enforcement of the kinematic conditions, but does not allow one to equate the element traction with the multipliers at a particular location within the element. The choice of function spaces does not require the interpolation for the multipliers to be continuous between elements. With a Lagrange multiplier method, though, the final matrix equations are semi-definite, and do not allow the multipliers to be eliminated at the element level. Thus, there is no computational advantage in choosing a discontinuous interpolation.

For the triangular element, the contact surface will be a curve in space. This implies that the contact interpolations will be the familiar Lagrange polynomials of order two defined on the canonical range (-1,1). Here too, Gaussian quadrature of sufficient order to exactly integrate straight-sided elements will be used to compute integrals of the matrices $\mathbf{q}$. The following section will detail the procedures for assembling these matrices for the discrete representation of the contact surface.

Contact Surface Calculations

Contact surface calculations can become a significant part of the computational effort during finite element analysis. It is essential that efficient means of contact detection be developed, and that these be optimized for either scalar, vector or parallel hardware. While the proposed method of discretizing the contact surface has been implemented only in two dimensions, it is readily extensible to three dimensions, and would suffer only from the naturally higher cost of three-dimensional geometric calculations. Several algorithms have been presented in the literature, including the pinball algorithm of Belytschko and Neal [37] and the contact segment treatment of Simo, Wriggers and Taylor [38]. Others have included the contact surface kinematics directly into a finite element formulation [41]. Laursen and co-workers have recently proposed a method which localizes all calculations to numerical quadrature points within finite elements on the contact surface [40,49]. This same algorithm was independently developed in the course of the present research.

Within an iterative cycle, three main tasks must be performed. First, given a point on one side of the contact surface, the closest point projection to the opposing surface is computed, and the finite element containing this projection is found. Second, utilizing the projection results, a discretized form of the contact surface is developed, which will be used in forming the contact matrices. Last, there is an assessment of changes to the surface, including points that come into or are released from contact. Each of these topics is covered in the remainder of this section.

In evaluating the Kuhn-Tucker relations the vector from a point on one surface directed normal to the opposing surface is required. This vector is referred to as the *gap function*, and, by construction, represents the minimum distance to the opposing surface. It has its origin at a *contactor point*, $\mathbf{x}_C$, located on a *contactor surface*, and terminates at the nearest point, $\mathbf{x}^*$, on a *target surface*. In the finite element context, this function will be evaluated with respect to the isoparametric coordinate interpolation and the current configuration of the contactor and target surfaces, represented by the deformed coordinates of finite element nodes on these surfaces.

Three pieces of data result from this calculation: the finite element which contains the closest point projection, the local coordinate of the projection within that element and the magnitude of the gap function. An algebraic sign is associated with the magnitude to indicate whether the contact point has penetrated the target surface. A positive magnitude represents surfaces which are not in contact. The sign is computed by comparing the direction of the gap function with that of the external normal to the contactor surface. The sign of the inner product of the normal vector with the gap function is taken as the sign of the magnitude, as illustrated in Fig. 2.

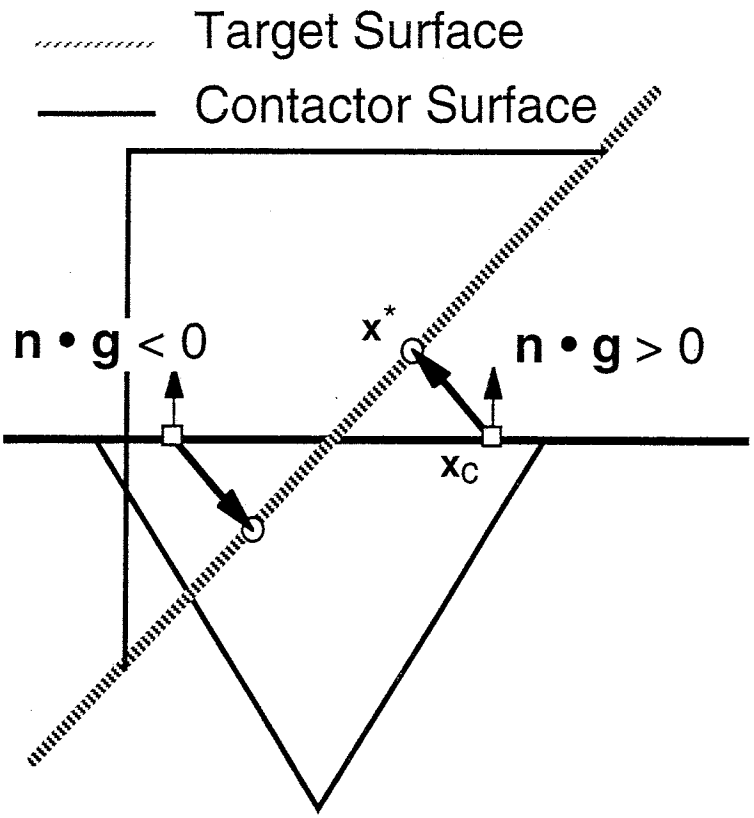

Fig. 2: Definition of the gap function and its sign on a contactor surface.

To initialize contact a user denotes model edges, in two dimensions, or model faces, in three dimensions, as *contactors* or *targets*. The finite element edges or faces that lie on those model entities then become contactor or target *segments*. A contactor segment may come in contact with a target, or several targets, in any part of the model. Arbitrarily, the contactor surface is associated with domain 'A' referred to in the problem definition, and the target surface is identified with domain 'B'.

The contact algorithm requires integrals to be performed along the contact surface. These integrals involve terms uniquely defined on the interface, and alternately, terms defined in the domain elements on either side of the contact surface. The discretization algorithm must provide a coordinate system in which to perform the integrals and information about the domain elements on either side. The most easily identified coordinate system is that which is already defined within the contactor segments. The nodes of the contact elements will therefore be chosen to coincide with those of the finite elements along the contactor surface. Interpolations of quantities associated with side 'A' of the contact surface are readily available, since the contact elements are aligned with the finite elements on the model boundary. Quantities associated with side 'B' can be computed in the finite element containing the closest point projection.

For each candidate contactor segment, an assessment must be made as to whether this segment should be included in the contact surface. Since the contact matrices will be integrated with numerical quadrature, this assessment is made for each quadrature point within the segment. Thus, the quadrature points also become the contactor points, $\mathbf{x}_C$, used to define the gap function. For each quadrature point two pieces of data are stored: the finite element into which it is projected and the local coordinate of the projected point. This data is the minimum required to perform the contact integrals and to define the degree-of-freedom connectivity for assembling the contact matrices.

Two other pieces of data are used to determine if this quadrature point should be considered active or not active for the contact integrals. These are the gap function and the normal component of total traction, calculated in the reference coordinates of the contactor segment. For quadrature points that were not previously active, they will be active in this iteration only if the gap is less than some positive tolerance. For quadrature points that were previously active, they will remain so if the normal component of total traction is negative and will be released if the traction is tensile. This constitutes the logic for an iterative procedure, where iterations within a time step continue until the solution quantities at the quadrature points agree with the assumed state.

Degrees-of-freedom for the Lagrange multipliers will be associated with the finite element nodes of the contactor segments. If at least one of the quadrature points within a contactor segment is classified as active, then the degrees-of-freedom are created for its nodes and are assigned unique numbers. To illustrate this refer to Eq. (20b) defining the element-level contact submatrix. When the index γ is taken to be 'A', the domain of the integral, Γ_{ce}, will be an entire contactor segment. Interpolations for the multipliers, **M**, are defined in the local coordinates of this contactor segment. Likewise, the surface normal, **n**, and velocity interpolations, **N**, can be computed by looking to the finite element associated with this contactor segment. In practice, each of these terms will be evaluated at some number of quadrature points along the contactor segment. In general, there is no direct correspondence between the local coordinates within a contactor segment and those within a *single* target segment. For this reason, contributions to both $\mathbf{q}^A$ and $\mathbf{q}^B$ are assembled on a per-quadrature-point basis. Thus, the contribution to $\mathbf{q}^A$ from the first active quadrature point in the contactor segment is computed and assembled into the global matrix. Then the contribution to $\mathbf{q}^B$ is calculated with respect to the finite element associated with the target segment containing the projection. Recall from the previous discussion that this closest point projection information has been stored for each quadrature point. This methodology allows for several interesting features including node-to-edge contact, partial contact within a contactor segment and multiple regions contacting at one point.

Validation Examples

The contact solutions developed by Hertz [50] are some of the only analytic results for evolving contact problems. As a demonstration of the discretization algorithm, the biphasic mixed-penalty contact finite element is used to solve the problem of a cylinder contacting an infinite medium. The problem is modeled in plane strain, and material parameters for the biphasic element must be chosen which will accurately simulate either rigid or linearly elastic materials. Figure 3 depicts the finite element mesh; there are 669 quadratic triangular elements and 1506 nodes, manually graded toward the contactor and target surfaces.

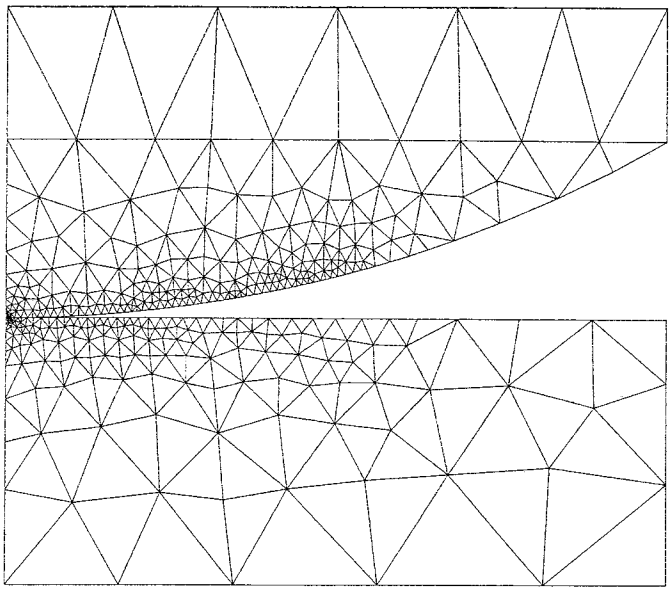

Fig. 3: Finite element mesh for the plane strain Hertz contact problem.

For this problem the flat surface of the foundation was chosen as the contactor and the curved surface of the cylinder was the target. Three combinations of materials are possible: both bodies elastic, an elastic cylinder contacting a rigid foundation or a rigid cylinder contacting an elastic foundation. Accurate solutions using a fixed mesh have been obtained for each case, demonstrating the invariance of the solution to the choice of contactor segments with regard to material properties and expected deformation. Results for the last case are presented here. The foundation is 2 mm in height and 5 mm in width, while the cylinder has a radius of 10 mm. Young's modulus for the foundation is 1.0 MPa and Poisson's ratio is 1/3. Both the cylinder and foundation are designated as 95% solid, and made highly permeable so there is no resistance to fluid flow. This essentially uncouples the solid and fluid motions and allows one to recover the compressible elastic solution from the biphasic theory. The penalty parameter is chosen as 1×10^{10} for the foundation. A rigid material is given material properties making it 1000 times stiffer than the compliant materials surrounding it.

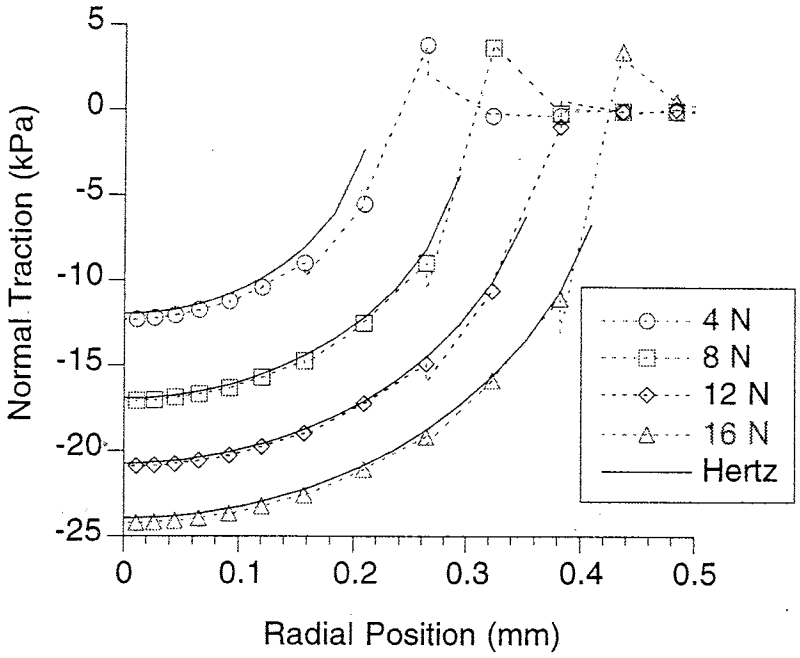

Fig. 4: Axial solid stress distributions for several applied loads in the plane strain Hertz contact problem.

While the elastic solution to Hertz contact is not time-dependent, the biphasic contact finite element formulation does discretize in time. For the elastic problem a force varying linearly with time is prescribed, and the solution at each time step is considered the elastic solution for that particular load level. Figure 4 compares the converged traction distributions, evaluated at the finite element nodes on the contactor surface, with the accepted solution at four load levels. As the load increases, the discretization algorithm continues to correctly predict the extent of the contact surface, and hence the traction distribution. The tensile traction at the edge of contact is due to partial contact within a contactor segment. In this case a single element is approximating both the steep gradient within the contact region and the traction-free condition outside the contact area. Mesh refinement would be required to more accurately define the edge of contact.

The previous example shows that the contact code is capable of finding the correct contact surface. The next goal is to verify the element for an evolving biphasic contact problem. There are limited solutions for this type of problem, an asymptotic solution presented by Ateshian *et al.* [51] and a more recent integral transform solution

by Kelkar and Ateshian [52]. The geometry is as in the plane strain Hertz contact problem, but with a height of 1mm, width of 20mm and indenter radius of 100mm. Physically the problem represents two identical cylinders layered with a biphasic material in contact along the length of their axes. Because of the symmetry, a geometrical transformation reduces this to a shallow, rigid, impermeable cylinder indented into a thin biphasic layer. A creep problem is modeled where a load is applied to the cylinder at $t = 0^+$ and held constant.

Following Kelkar's model, the solid phase Lamé parameters for the tissue layer are $\lambda = 0.0$, $\mu = 0.25$MPa; the solid volume fraction is $\phi^s = 0.25$; the tissue permeability is $\kappa = 0.2\times10^{-14}$ m^4/Ns; and the penalty parameter is $\beta = 1.0\times10^{10}$. A distributed load equal to 1000N is applied to the rigid cylinder in one time step. Results are presented for times well beyond the application of load. This allows for differences between a true step load and the short ramp loading to decay. Figure 5 shows excellent agreement between the surface normal traction predicted by the integral transform solution (lines) and the finite element solution (symbols) at $t = 100$s. Similar correlations are observed for times from 20 to 200 seconds, and for kinematic variables. Observe that the fluid traction is nearly twice the solid traction. At much longer times, when fluid flow ceases, the pressure will be zero and the total load will be carried by the solid phase.

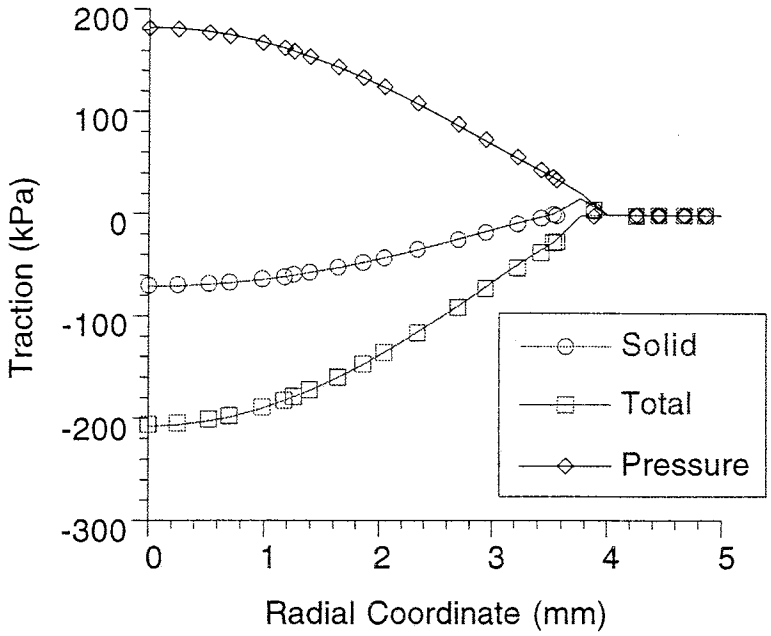

Fig. 5: Normal traction distributions for biphasic indentation after 100 seconds of creep. Lines are the integral transform solution and symbols are the finite element result.

In Fig. 6, note how the tissue surface has undergone a tensile deformation in the outer portion of the contact surface, also at t = 100s. This region also experiences an efflux of fluid, as depicted by the relative velocity. The maximum principal stress is shown as a shaded contour on a mesh deformed by five times the displacement; the scale is given in kilopascals at right. The magnitude and direction of the relative velocity field is indicated by arrows, with magnitudes ranging to 0.43 μm/s.

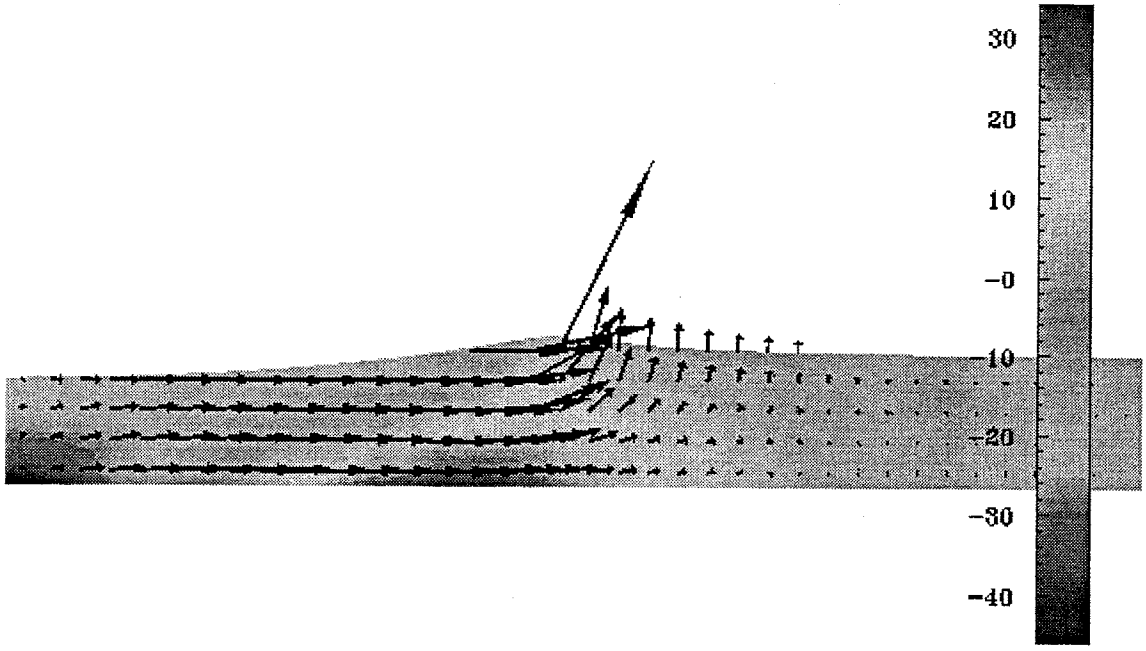

Fig. 6: Shaded contour of maximum principal stress in kPa for biphasic indentation. Solutions are on a 5× deformed mesh after 100 seconds of creep. The relative velocity field is indicated by arrows.

Summary

With the success of the first biphasic contact finite element formulation, several opportunities to increase the sophistication of diarthrodial joint modeling become apparent. The single most important tool in developing a complete simulation of articulation is three-dimensional finite element analysis of contact. While the present formulation could be implemented with a three-dimensional element, several other enhancements are required to make this element useful in clinically relevant problems.

Certainly paramount are finite deformation and material nonlinearity. Large-displacement, sliding contact, which is observed in every diarthrodial joint, cannot be modeled within the confines of geometric linearity. The material non-linearities represent tissue behaviour which is observed during *in vitro* tissue tests, and must be included in the model to obtain a physically meaningful solution. The effects of material and geometric linearity have been included in recent work by Almeida [32]. In the course of that research, two- and three-dimensional elements have been implemented for the mixed-penalty and velocity-pressure formulations. It is possible that

frictional effects on the contact surface play an important role in the overall deformational behaviour. Additional experimental research is required to quantify this effect and to postulate the laws that may govern it for tissue mechanics [53].

Any numerical analysis technique should be capable of providing some measure of the error in the numerical approximation. For the examples presented here, this has been the traditional approach of a convergence study; the finite element mesh is refined until solutions on subsequent meshes are the same. In the future the biphasic contact finite element should be coupled with error estimation techniques and automatic mesh enrichment. Error estimates for parabolic system of equations have been developed (see, for example, [54-57]), and research has been conducted on error analysis for porous soils using Biot's equations [58,59]. A research effort focused on extending these error estimates specifically to the linear and nonlinear forms of the biphasic theory is necessary. This must be coupled to related work on *h*, *p* or *h-p* adaptivity.

Acknowledgments

The authors wish to acknowledge the support of the National Science Foundation through grant ASC-9318184. We also thank Prof. M. S. Shephard for his comments during the course of the research and for making available the resources of the Scientific Computation Research Center at Rensselaer.

References

[1] H. Lipshitz and M. J. Glimcher, In vitro studies of the wear of articular cartilage: II. Characteristics of the wear of articular cartilage when worn against stainless steel plates having characterized surfaces, Wear 52 (1979) 297-339.

[2] L. L. Malcom, An experimental investigation of the frictional and deformational response of articular cartilage interfaces to statistic and dynamic loading, Ph.D. thesis (Univ. of California, San Diego, 1976).

[3] C. A. McDevitt, E. Gilbertson and H. Muir, An experimental model of osteoarthritis: early morphological and biochemical changes, J. Bone Jt. Surg. 59B (1977) 24-35.

[4] V. C. Mow, L. A. Setton, D. S. Howell and J. A. Buckwalter, Structure-function relationship of articular cartilage and the effect of joint instability and trauma on cartilage function, in: K. D. Brandt, ed., Cartilage Changes in Osteoarthritis (University of Indiana Press, Indianapolis IN, 1990) 22-42.

[5] V. C. Mow, S. C. Kuei, W. M. Lai and C. G. Armstrong, Biphasic creep and stress relaxation of articular cartilage in compression: theory and experiments, J. Biomech. Engng. 102 (1980) 73-84.

[6] K. A. Athanasiou, A. Agarwal and G. Constantinides, Creep Indentation of Human Hip Articular Cartilage: Comparisons of Biphasic Finite Element/Optimization and Semi-Analytical Solutions, in: M. W. Bidez, ed., ASME Winter Annual Meeting (ASME, Anaheim, CA, 1992) 195-198.

[7] T. D. Brown and R. J. Singerman, Experimental determination of the linear biphasic constitutive coefficients of human fetal proximal femoral chondroepiphysis, J. Biomech. 10 (1986) 597-605.

[8] J. A. Favenesi, J. C. Shaffer and V. C. Mow, Biphasic mechanical properties of knee meniscus, Trans. Orthop. Res. Soc. 8 (1983) 57.

[9] M. K. Kwan, W. M. Lai and V. C. Mow, A finite deformation theory for cartilage and other soft hydrated connective tissues, J. Biomech. 23 (1990) 145-155.

[10] V. C. Mow, M. K. Kwan, W. M. Lai and M. H. Holmes, A finite deformation theory for nonlinearly permeable cartilage and other soft hydrated connective tissues, in: S. L.-Y. Woo, G. Schmid-Schonbein and B. Zweifach, ed., Frontiers in Biomechanics (Springer-Verlag, New York, 1986) 153-179.

[11] W. M. Lai and V. C. Mow, Drag-induced compression of articular cartilage during a permeation experiment, Biorheol. 17 (1980) 111-123.

[12] W. M. Lai, V. C. Mow and V. Roth, Effects of nonlinear strain-dependent permeability and rate of compression on the stress behavior of articular cartilage., J. Biomech. Engng. 103 (1981) 61-66.

[13] M. H. Holmes, W. M. Lai and V. C. Mow, Singular perturbation analysis of the nonlinear, flow-dependent compressive stress relaxation behavior of articular cartilage, J. Biomech. Engng. 107 (1985) 206-218.

[14] B. Cohen, Anisotropic hydrated soft tissues in finite deformation and the biomechanics of the growth plates, Ph. D. thesis (Columbia University, 1992).

[15] A. F. Mak, The apparent viscoelastic behavior of articular cartilage-The contributions from the intrinsic matrix viscoelasticity and interstitial fluid flows, J. Biomech. Engng. 108 (1986) 123-130.

[16] L. A. Setton, W. B. Zhu and V. C. Mow, The biphasic poroviscoelastic behavior of articular cartilage: Role of the surface zone in governing the compressive behavior, J. Biomech. 26 (1993) 581- 592.

[17] J. T. Oden and H. Kikuchi, Finite element methods for constrained problems in elasticity, Int. J. Num. Meth. in Engng. 18 (1982) 701-725.

[18] D. S. Malkus and T. J. R. Hughes, Mixed finite element methods - reduced and selective integration techniques: A unification of concepts, Comp. Meth. Appl. Mech. Engng. 15 (1978) 63-81.

[19] R. L. Spilker and J.-K. Suh, Formulation and evaluation of a finite element model of soft hydrated tissue, Computers and Structures 35 (1990) 425-439.

[20] J.-K. Suh, R. L. Spilker and M. H. Holmes, A penalty finite element analysis for nonlinear mechanics of biphasic hydrated soft tissue under large deformation, Int. J. Num. Meth. in Engng. 32 (1991) 1411-1439.

[21] R. L. Spilker and T. A. Maxian, A mixed-penalty finite element formulation of the linear biphasic theory for soft tissues, Int. J. Num. Meth. in Engng. 30 (1990) 1063-1082.

[22] M. E. Vermilyea and R. L. Spilker, A hybrid finite element formulation of the linear biphasic equations for soft hydrated tissues, Int. J. Num. Meth. in Engng. 33 (1992) 567-594.

[23] C. W. J. Oomens, D. H. Van Campen and H. J. Grootenboer, A mixture approach to the mechanics of skin, J. Biomech. 20 (1987) 877-885.

[24] J. S. Wayne, S. L.-Y. Woo and M. K. Kwan, Application of the u-P finite element method to the study of articular cartilage, J. Biomech. Engng. 113 (1991) 397-403.

[25] J.-K. Suh, A finite element formulation for nonlinear behavior of biphasic hydrated soft tissue under finite deformation, Ph.D. thesis (Rensselaer Polytechnic Institute, 1989).

[26] T. A. Maxian, A six-node triangular element for the mixed-penalty finite element formulation of the linear biphasic theory, Master of Science thesis (Rensselaer Polytechnic Institute, 1989).

[27] R. L. Spilker, E. S. Almeida, C. Clutz, M. S. Shephard, G. A. Ateshian and P. S. Donzelli, Three dimensional automated biphasic finite element analysis of soft tissues from stereophotogrammetric data, in: J. M. Tarbell, ed., 1993 Advances in Bioengineering (ASME, New York, 1993) 15-18.

[28] R. L. Spilker, M. S. Shephard, G. A. Ateshian, V. C. Mow, E. S. Almeida, P. S. Donzelli and C. J. Clutz, Simulating the 3D biphasic response of soft tissues in diarthrodial joints using physiological data, in: L. Blankevoort and J. G. M. Kooloos, ed., Second World Congress of Biomechanics (Stichting World Biomechanics, Nijmegen, 1994) 212.

[29] M. S. Shephard and M. K. Georges, Automatic three-dimensional mesh generation by the finite octree technique, Int. J. Num. Meth. in Engng. 32 (1991) 709-739.

[30] P. S. Donzelli, R. L. Spilker, P. L. Baehmann, Q. Niu and M. S. Shephard, Automated adaptive analysis of the biphasic equations for soft tissue mechanics using a posteriori error indicators, Int. J. Num. Meth. in Engng. 34 (1992) 1015-1033.

[31] J. R. Booker and J. C. Small, An investigation of the stability of numerical solutions of Biot's equations of consolidation, Int. J. Solids Structures 11 (1975) 907-917.

[32] E. Almeida, Finite Element Formulations for Biological Soft Hydrated Tissues Under Finite Deformation, PhD thesis (Rensselaer Polytechnic Institute, 1995).

[33] P. L. Baehmann and M. S. Shephard, Adaptive multiple-level h-refinement in automated finite element analysis, Engng. Comp. 5 (1989) 235-247.

[34] K. L. Johnson, Contact Mechanics (Cambridge University Press, New York, 1985).

[35] N. Kikuchi and J. T. Oden, Contact Problems in Elasticity: A Study of Variational Inequalities and Finite Element Methods (Society for Industrial and Applied Mathematics, Philadelphia, 1988).

[36] P. Wriggers, T. V. Van and E. Stien, Finite element formulation of large deformation impact-contact problems with friction, Comp. & Struct. 37 (1990) 319-331.

[37] T. Belytschko and M. O. Neal, Contact-impact by the pinball algorithm with penalty and Lagrangian methods, Int. J. Num. Meth. in Engng. 31 (1991) 547-572.

[38] J. C. Simo, P. Wriggers and R. L. Taylor, A perturbed Lagrangian formulation for the finite element solution of contact problems, Comp. Meth. Appl. Mech. Engng. 50 (1985) 163-180.

[39] J. C. Simo and T. A. Laursen, An augmented Lagrangian treatment of contact problems involving friction, Comp. & Struct. 42 (1992) 97-116.

[40] T. A. Laursen and V. G. Oancea, Automation and assessment of augmented lagrangian algorithms for frictional contact problems, J. Appl. Mech. (1995)

[41] J.-H. Heegaard and A. Curnier, An augmented lagrangian method for discrete large-slip contact problems, Int. J. Num. Meth. in Engng. 36 (1993) 569-593.

[42] J.-H. Heegaard, Large slip contact in biomechanics: kinematics and stress analysis of the patello-femoral joint, Ph. D. thesis (Ecole Polytechnique Federale de Lausanne, 1993).

[43] J. S. Hou, M. H. Holmes, W. M. Lai and V. C. Mow, Boundary conditions at the cartilage-synovial fluid interface for joint lubrication and theoretical verifications, J. Biomech. Engng. 111 (1989) 78-87.

[44] P. S. Donzelli, A Mixed-Penalty Contact Finite Element Formulation for Biphasic Soft Tissues, PhD thesis (Rensselaer Polytechnic Institute, 1995).

[45] R. T. Haftka, Z. Gurdal and M. P. Kamat, Elements of Structural Optimization (Kluwer Academic Publishers, Dordrecht, the Netherlands, 1990).

[46] M. S. Engelman, R. L. Sani, P. M. Gresho and M. Bercovier, Consistent vs. reduced integration penalty methods for incompressible media using several old and new elements., Int. J. Num. Meth. Fluids 2 (1982) 25-42.

[47] O. C. Zienkiewicz and R. L. Taylor, The Finite Element Method (McGraw-Hill Book Company, London, 1989).

[48] T. J. R. Hughes, The Finite Element Method Linear Static and Dynamic Analysis (Prentice-Hall, Inc., Englewood Cliffs, 1987).

[49] T. A. Laursen and J. C. Simo, A continuum-based finite element formulation for the implicit solution of multibody, large deformation frictional contact problems, Int. J. Num. Meth. in Engng. 36 (1993) 3451-3485.

[50] H. Hertz, Uber die beruhrung fester elastischer korper, J. f. Math. (Crelle) 92 (1881)

[51] G. A. Ateshian, W. M. Lai, W. B. Zhu and V. C. Mow, An asymptotic solution for two contacting biphasic cartilage layers, J. Biomech. 27 (1994) 1347-1360.

[52] R. Kelkar and G. A. Ateshian, Contact creep response between a rigid impermeable cylinder and a biphasic cartilage layer using integral transforms, in: R. M. Hochmuth, N. A. Langrana and M. S. Hefzy, ed., 1995 Bioengineering Conference (ASME, New York, 1995)

[53] G. A. Ateshian, A theoretical model for boundary friction in articular cartilage, in: G. T. Yang, K. Hayashi, S. Y.-L. Woo and J. C. H. Goh, ed., Proceedings of the 4th China-Japan-USA-Singapore Conference on Biomechanics (International Academic Publishers, 1995) 142-145.

[54] P. K. Moore and J. E. Flaherty, Adaptive local overlapping grid methods for parabolic systems in two space dimensions, J. Comp. Phys. 98 (1992) 54-63.

[55] S. Adjerid, J. E. Flaherty, P. K. Moore and Y. Wang, High-order adaptive methods for parabolic systems, Phys. D. 60 (1992) 94-111.

[56] C. Johnson, Numerical Solution of Partial Differential Equations by the Finite Element Method (Cambridge University Press, Cambridge, 1987).

[57] C. Johnson, Adaptive finite element methods for diffusion and convection problems, Comp. Meth. Appl. Mech. Engng. 82 (1990) 301-322.

[58] M. A. Murad and A. F. D. Loula, Improved accuracy in finite element analysis of Biot's consolidation problem, Comp. Meth. Appl. Mech. Engng. 95 (1992) 359-382.

[59] M. A. Murad and A. F. D. Loula, On stability and convergence of finite element approximations of Biot's consolidation problem, Int. J. Num. Meth. in Engng. 37 (1994) 645-667.